Biomolecular and electrochemical charge detection by a micromechanical electrometer

Andreas Menzel[a,b], Angel T.-H. Lin[a], Pedro Estrela[c], Peng Li[a], Ashwin A. Seshia[a,*]

[a] *Department of Engineering, University of Cambridge, Trumpington Street, Cambridge CB2 1PZ, UK*

[b] *Department of Microsystems Engineering - IMTEK, University of Freiburg, Georges-Koehler-Allee 103, 79110 Freiburg, Germany*

[c] *Department of Electronic and Electrical Engineering, University of Bath, Bath BA2 7AY, UK*

**Corresponding author: Tel: +44 (0)1223 760333 Fax: +44 (0)1223 760309*

E-mail address: aas41@cam.ac.uk

Abstract:

A micromechanical electrometer is applied to the label-free detection of biomolecular interactions and electrochemical charge sensing. The primary element of the electrometer is a micromechanical variable capacitor to modulate and convert a dc charge to an ac voltage output, thereby limiting the effects of low frequency noise on charge detection. At room temperature and ambient pressure the noise-limited charge resolution of a micromechanical electrometer based on this principle is found to be 3 $e/\sqrt{Hz}$, enabling the potential detection of charged single molecule binding on electrode surfaces. The detection principle is validated by several experiments. Biomolecular binding experiments are conducted on an external gold electrode situated within a custom-designed flow cell and electrically connected to the micromachined electrometer. The concepts are validated by demonstrating the detection of biotin-streptavidin binding and DNA hybridization. Furthermore, it is shown that the electrometer can be applied for the detection of the redox system ferrocyanide/ferricyanide to describe Nernstian behaviour due to well defined charge transfer on the electrode surface at different concentration ratios as expected.

Keywords: MEMS, electrometer, charge detection, label-free biosensor

1. Introduction:

Biosensors based on the electrical detection of molecular charge have a role to play in enabling the next-generation of portable parallel bio-analyte detection. There are several examples of transducers used in charge sensing of biomolecular interactions. An example of this type of electrochemical transducer is the ion-sensitive field effect transistor (ISFET) that can also be employed to detect biomolecular interactions on functionalized gate electrodes [1]. The measured drain current of an ISFET has a dependency on charge, built up at the gate-connected electrode due to molecular binding [2]. Other common principles adopted for label-free biological detection include mechanical sensors based on the modulated self-resonance of a vibrating structure and modulation of acoustic wave transport in solid and solid/liquid interfaces, where resonant frequency shift can serve as a characteristic for a change in mass. Examples of such devices include the quartz crystal microbalance (QCM) [3], surface acoustic wave (SAW) [4] as well as film bulk acoustic resonators (FBAR) [5]. A further approach for mechanical detection of biochemical interactions uses microcantilevers where biomolecular interactions induce a bending in the mechanical structure. While there is ongoing investigation into the source of mechanical bending, various studies have shown that electrostatic interactions generated by molecular binding to the cantilever surface plays a role in defining static mode bending response [6] and resonant frequency response in dynamic mode [7].

In this paper, we describe the concept of detecting biomolecular interactions based on high resolution charge sensing instruments called electrometers. In terms of small-scale electrometers, a torsion-balanced electrometer has been reported to achieve a sensitivity of ~ 0.1 $e/\sqrt{Hz}$ [8], and a non-linear regime operating nanomechanical resonator was described with a sensitivity of ~ 0.1 $e/\sqrt{Hz}$ [9]. However, these devices are operated at very low temperatures (~ 4.2 K) and vacuum

conditions to meet this resolution and are somewhat limited in terms of dynamic range. In order to operate in room temperature (23 °C) and atmospheric pressure, a vibrating reed electrometer based on micro electro mechanical systems (MEMS) was reported with a resolution of ~ 51 $e/\sqrt{Hz}$ by [10] and a resolution in the sub-10 electron regime was subsequently demonstrated by [11] based on the same principle.

The electrometer reported here is an extension of the work previously reported by our group [11]. This electrometer translates charge to voltage using a modulated variable capacitor driven a given frequency, while the output signal is measured at twice the drive frequency. In this paper, the approach for detecting biomolecular interactions relies on connecting the charge-transfer electrode in an appropriately designed electrochemical flow setup to the micromechanical variable capacitor of the electrometer. For demonstration of the detection mechanism, several model systems were studied: electrochemical redox couples, binding of biotin with streptavidin, and DNA hybridization. In the approach presented here, an electrode surface is functionalized with a specific biological recognition element on a self assembled monolayer (SAM). Biotin was used for streptavidin recognition and single stranded DNA (ssDNA) probes for detection of DNA hybridization.

2. Materials and methods:

2.1 Electrometer modeling:

The total capacitance of the electrometer is modeled by a variable capacitor realized by a vibrating movable shuttle and a parasitic capacitance, which is given by all the interface parasitic capacitances between sensor output and readout electronics. A derivation of all necessary equations has already been described elsewhere [11]. The movable shuttle is vibrating with

mechanical vibration amplitude and a harmonic excitation frequency. Applying a defined charge to the input terminal of the variable sense capacitance will yield to a corresponding sensor voltage change containing only even harmonics. The second harmonic signal provides the largest response of the output rms voltage ($V_{out,rms}$) with respect to the input charge (Q_{in}). An expression of the rms responsivity ℜrms is described in equation 1 with C_S and C_P as the sensing and parasitic capacitances while X the vibration amplitude of the movable shuttle and g the equally distanced gaps of the parallel plate sense capacitances describe. The responsivity, ℜrms, is found by a suitable calibration procedure discussed below.

$$\Re_{rms} = \frac{\partial V_{out,rms}}{\partial Q_{in}} = \frac{C_S}{2\sqrt{2}(C_S + C_P)}\left(\frac{X}{g}\right)^2 \quad (1)$$

2.2 Instrumentation:

Gold electrodes with an area of 0.635 cm × 0.635 cm were used as the active sensor surface. The gold electrodes are mounted in a specially designed flow cell that isolates the electrodes and fluid medium. The flow cell system also contains an Ag/AgCl reference electrode to realize a measurement with respect to the system ground. The electrode and flow cell are mounted onto a printed circuit board (PCB), which is directly connected to the on-chip MEMS electrometer device (see figure 1a and 1b). The PCB also integrates the drive electronics for the electrometer structure, and the readout electronics. The electrometer device is fabricated as a suspended silicon structure in a silicon-on-insulator (SOI) foundry process. A SEM micrograph of the fabricated device is shown in figure 2. The system is driven into resonance electrically using comb drive structures (dc bias voltage V_{bias} and ac voltage V_{ac}), and parallel plates are used to realize a variable sensing capacitor. The electrometer output was conditioned by a low-noise amplifier and then displayed on

a spectrum analyzer. All the measurements were performed by operating the electrometer device at room temperature and ambient pressure.

An estimation of the amount of charge applied at the sense electrode (due to molecular binding on electrode surfaces) can be determined by measuring the steady state second harmonic voltage amplitude (charge modulation) before and after a reaction has been taken.

2.3 Chemicals:

DNA oligonucleotides were purchased from IBA GmbH, while the biotin samples were obtained from Pierce. All other chemicals were purchased from Sigma-Aldrich. Prior to functionalization, Au electrodes were cleaned by rinsing with acetone, isopropanol, deionized water and dissociating any remaining organic contaminants by adsorbing a short UV radiation. For the electrochemical redox marker experiments, a SAM was formed on the Au electrodes by exposing them to 10 mM mercaptohexanol (MCH) in absolute ethanol for 1 hour. The SAM layer covers the Au surface, protecting it from undesirable ionic adsorption. To obtain varying redox-defined potentials, the ratio of oxidized to reduced concentrations (c_{ox}/c_{red}) of the redox couple $[Fe(CN)_6]^{4-/3-}$ was varied in concentrations between 100 µM and 100 mM by dissolving the appropriate amounts of potassium ferrocyanide $K_4[Fe(CN)_6]$ and potassium ferricyanide $K_3[Fe(CN)_6]$ in a 10 mM phosphate buffered saline (PBS) charge carrier buffer (prepared using PBS tablets procured from Sigma Aldrich).

For the protein interaction studies, Au electrodes were exposed to 1 mM N-(6(biotinamido)hexyl)-3'-(2'-pyridyldithio)-propioinamide (biotin-HPDP) in ethanol for 2.5 hours. Control experiments were performed with Au electrodes functionalized with 2 mM

methoxy polyethylene glycol (mPEG) in ethanol for 2.5 h [12]. Samples were rinsed in water after the immobilization procedure. Binding experiments were performed with streptavidin from Streptomyces avidinii diluted into a 100 mM phosphate buffer (PB) solution (NaH_2PO_4 and Na_2HPO_4). All measurements and sample preparation were performed in PB with pH 7.1. A verification of the biotin-HPDP surface coverage and correspondent bound streptavidin surface density using this procedure has been demonstrated earlier [12] where AFM measurements of functionalized surfaces was performed for the same surface preparation protocols.

For the DNA hybridization experiments, a mixed SAM of 10 µM MCH and 1 µM of 5'thiolated 26-base ssDNA oligonucleotides was immobilized on the Au electrodes. The sequence of the ssDNA probe was HS-$(CH_2)_6$-5' CAT TAA TGC TAT GCA GAA AAT CTT AG 3'. Immobilization was performed for 12 h in a high ionic strength pH 7.1 buffer of 0.8 M phosphate buffer (PB), 1 M potassium sulfate (K_2SO_4), 5 mM magnesium chloride ($MgCl_2$) and 5 mM ethylene diamine tetraacetic acid (EDTA). This high ionic strength and the Mg^{2+} ions screen the DNA charge, allowing for high probe densities on the surface due to the short Debye length. After immobilization, the electrode was rinsed with the ionic strength buffer, followed by 200 mM PB with 10 mM EDTA, and finally 10 mM PB. EDTA is used to create a metal complex for removing any remaining Mg^{2+} ions. To ensure the thiol coverage on the surface is complete, an additional 1 mM MCH step was performed to backfill the remaining spaces of potentially non covered areas [13]. Hybridization measurements were performed in a buffer containing 50 mM PB and 100 mM K_2SO_4 with 1 µM complementary DNA strands, 5' CTA AGA TTT TCT GCA TAG CAT TAA TG 3' or non-complementary strands, 5' CAT TAA TGC TAT GCA GAA AAT CTT AG 3'.

2.4 Sample characterization:

Before measuring the different reactions on the Au samples, the MEMS electrometer was characterized. The electrometer was differentially driven into resonance by applying a dc bias of V_{bias}=31 V and an ac voltage of V_{ac}=4 V to the comb drive structure. The resonant frequency was identified to be 3.6 kHz. The second harmonic rms voltage amplitude V_{out} at 7.2 kHz is measured using a spectrum analyzer after buffering and amplifying the signal on a purpose-designed PCB. The calibration of the electrometer is done by supplying defined values of electrical charge using an integrated on-chip calibration capacitor on charge sensing node of the vibrating electrometer. The functionalized electrode samples were mounted into the flow cell and connected to the electrometer. Initially, the signal is measured with the flow cell filled with measurement buffer. After reaching a steady state, the measurand (redox couples, proteins or DNA, respectively) was injected into the flow cell and the electrode signal was measured again during the reaction process and after equilibration.

3. Results and Discussion:

Initially, a calibration of the electrometer device is performed by loading the sense electrodes successively with charges between -236 fC and 236 fC and monitoring the second harmonic rms voltage. This calibration step is performed without any electrode and flow cell configuration (see figure 3). The derivative with respect to the input charge Q_{in} (according to equation 1) of the best fit line to the data results in a responsivity of 25.11×10^{10} V/C and a charge noise floor of ~ 3 e/$\sqrt{Hz}$ limited by the input electronics noise (12 nV/$\sqrt{Hz}$) of the front-end buffer amplifier. The obtained charge noise floor is an improvement compared to 6 e/$\sqrt{Hz}$ [11] and is mainly achieved by reducing the parasitic on chip and circuit capacitances C_p. A similar procedure was performed

including the flow cell and electrode configuration which was filled with 100 mM PB and a responsivity of 4.7261×10^5 V/C was found.

For demonstrating the electrometer concept by detecting specific defined charge transfer on the electrode surface, the redox couple system was chosen. The redox couple given by ferrocyanide and ferricyanide provides a reduced form Fe^{2+} (c_{red}) and oxidized form Fe^{3+} (c_{ox}) and can change the redox potentials in solution by varying the concentration ratios c_{ox}/c_{red}. This, in turn, affects the electrode surface charge resulting in an electrometer response. Initially, a 10 mM PBS buffer was injected into the flow cell and a base line was measured. Upon injection of a ratio of 100 µM to 100 µM (1:1) redox couple in a 10 mM PBS, the sensor's response signal was observed to change as shown in the inset of figure 4. The concentration ratio was successively increased from 1 to 1000 and monitored over time. The corresponding sensor output signals (figure 4, blue line and measurement points) indicate a Nernstian behaviour as shown by the best fit line in a V_{out} vs. c_{ox}/c_{red} plot (see figure 4, red line). With help of responsivity data, a double layer capacitance of 46 µF can be calculated, which is 30-50 times larger than what has been reported in the literature [14].

Next, the detection of biotin-streptavidin binding is demonstrated [15]. The experiments were performed in the flow cell with mPEG functionalized electrode surfaces (inset of figure 5a, red curve). A base line in a PB buffer solution was taken over a time of 10 minutes. A streptavidin concentration of 20 nM was injected into the flow cell system and incubated on the functionalized surface for 30 minutes. The streptavidin solution was rinsed away with 100 mM PB and measured in the same 100 mM PB solution. As it can be seen, the electrometer is relatively insensitive to streptavidin using this protein resistive mPEG coating. The mPEG coating hinders the non-specific adsorption of proteins and can therefore be used for reference measurements. Next, an

electrometer measurement with biotin-HPDP functionalized surface is performed. Under the same conditions, 20 nM streptavidin was injected after establishing a buffer baseline in 100 mM PB. Streptavidin was incubated for 30 minutes and rinsed away with 100 mM PB measurement buffer (inset of figure 5a, blue curve). The blue curve exhibits an additional noise behavior and artifacts which can be deduced to the low target concentration and the superposed noise generated by the measurement buffer solution.

After this initial test measurement, similar measurements were performed to obtain a concentration profile measurement for different streptavidin concentrations reacting with biotin-HPDP SAM surfaces. Streptavidin concentrations in 10 nM, 20 nM, 50 nM and 100 nM in a 100 mM PB buffer solution were used. Initially, 100 mM PB was injected in the into the flow cell with the fresh prepared biotinylated exposed electrode and a stabilized baseline was measured for 30 minutes. Next, the PB buffer solution consisting of different concentrations of streptavidin were successively injected into the flow cell system and incubated for 30 minutes, rinsed and measured with 100 mM PB measurement buffer. The measured steady states after rinsing with PB were detected and from the previously recorded steady state lines subtracted. Assuming uniform binding, the concentration profile can be converted into estimated number of proteins per unit area as shown in figure 5a. The estimated protein density varies between 9.37×10^{8} proteins/cm^2 for 10 nM and 19.85×10^{9} proteins/cm^2 for 100 nM. Fitting the data yields the typical behavior of a Langmuir adsorption isotherm. However, a density in the range of 10^{12} proteins/cm^2 has been reported by SPR and QCM measurements. The obtained reaction constant K_A of 2.65×10^{7} mol^{-1} is quite low, which may result from limited transport and diffusion processes in the bulk solution during the incubation. The deviations in the data might be explained by to the surface roughness and purity of the Au surface. The spacer arm of the disulfide group to the biotin ring is 29.2 Å [16]

and the size of streptavidin is in the range of ~5 nm [17]. In our case, the Au electrode has a surface roughness larger than 10 nm which could result in increased hindrance for protein transport to the surface and in binding to the reactive biotin molecule. In future work, experiments with lower surface roughness should be conducted to minimize these limitations and improve the binding affinity.

Further tests have been carried out with DNA to demonstrate charge detection during DNA hybridization [18]. Figure 5b depicts the process when hybridizing complementary and non-complementary DNA strands to ssDNA probe functionalized surfaces. For both experiments, a baseline for the functionalized electrode is first established in measurement buffer.

Next, the ssDNA modified gold surface was exposed to 1 μM of non-complementary ssDNA and measured (see red curve in figure 5). Only a small change in electrometer signal can be seen after rinsing and measuring with measurement buffer since the non-complementary strands do not bind to the probe ssDNA. The opposite effect is shown in the blue curve of figure 5b where a complementary sequence was injected into the flow cell and the signal magnitude was seen to change drastically. The measured steady state signal difference before and after the hybridization step was $|\Delta V_{out}|$ = 7.53 mV and using the calibrated responsivity yields an estimated molecular binding density of approximately 9.5×10^{9} DNA molecules/cm^2. Further experiments have shown that 10 nM target ssDNA is detectable and this can also seen by comparing the signal-to-background in figure 5b. Further optimization may be achieved by low-parasitic electrode-circuit integration, improved gold surface quality and SAM surface packing density.

4. Conclusions

The implementation of a micromechanical electrometer for biomolecular and electrochemical charge detection was successful demonstrated. The MEMS electrometer was shown to operate for typical examples such as redox couples to detect a potential in an electrochemical system as well as the detection of biotin-streptavidin binding and DNA hybridization. The challenge of detecting charge on an Au electrode has been addressed by developing a flow cell system containing a working electrode connected to the MEMS electrometer sense capacitor input and a reference Ag/AgCl wire as a reference with respect to system ground. The electrochemical redox experiment was shown to follow a Nernstian behaviour, when changing the redox states in the flow cell. The interaction of biotin-streptavidin was also detectable and the usage of a protein resistant monolayer, such as mPEG SAM is successfully employed as a reference for streptavidin binding to the surface. DNA hybridization detection is demonstrated with clear distinction between the binding of complementary and non-complementary ssDNA on the immobilized surface. These experiments taken together present a proof-of-concept adaptation of a micromechanical electrometer for the biomolecular charge detection. Further efforts to optimize the design of the system, including the coupling of the electrical detection to the detection electrode and the quality of the gold films together with improved binding density on the surface could realize the promise for highly sensitive detection of electrode surface interactions.

Acknowledgments

This work was supported in part by the US Army Soldier Systems Center. The authors thank Mrunal Khaderbad for help with the SEM micrographs and Joshua Lee for his notes on the electrometer design and calibration.

References:

[1] Estrela, P., Stewart, A.G., Yan, F., Migliorato, P., Field effect detection of biomolecular interactions, Electrochim. Acta, 50 (2005), 4995-5000.

[2] Kim, D.-S., Park, J.-E., Shin, J.-K., Kim, P.-K., Lim, G., Shoji, S., An extended gate FET-based biosensor integrated with a Si microfluidic channel for detection of protein complexes, Sens. Actuators, B, 117 (2006), 488–494.

[3] Marx, K., Quartz crystal microbalance: A useful tool for studying thin polymer films and complex biomolecular systems at the solution-surface interface, Biomacromolecules 4 (2003), 1099–1120.

[4] Länge, K., Bender, F., Voigt, A., Gao, H., Rapp, M., A surface acoustic wave biosensor concept with low flow cell volumes for label-free detection, Anal. Chem. 75 (2003), 5561–5566.

[5] Nirschl, M., Bluher, A., Erler, C., Katzschner, B., Vikholm-Lundin, I., Auer, S., Voros, J., Pompe, W., Schreiter, M., Mertig, M., Film bulk acoustic resonators for DNA and protein detection and investigation of in vitro bacterial s-layer formation. Sens. Actuators, A 156 (2008), 180–184.

[6] Berger, R., Delamarche, E., Lang, H., Gerber, C., Gimzewski, J., Meyer, E., Guntherodt, H.-J., Surface stress in the self-assembly of alkanethiols on gold, Science 276 (1997), 2021–2024.

[7] Thundat, T., Warmack, R., Chen, G., Allison, D., Thermal and ambient-induced deflections of scanning force microscope cantilevers, Appl. Phys. Lett. 64 (1994), 2894.

[8] Cleland, A. N., Roukes, M. L., A nanometer-scale mechanical electrometer, Nature 392 (1998), 160–162.

[9] Krömmer, H., Erbe, A., Tilke, A., Manus, S., Blick, R. H., Nanomechanical resonators operating as charge detectors in the nonlinear regime, Europhys. Lett. 50 (2000), 101–106.

[10] Riehl, P. S., Scott, K. L., Muller, R. S., Howe, R. T., Yasaitis, J. A., Electrostatic charge and field sensors based on micromechanical resonators, J Microelectromech S 12 (2003), 557–589.

[11] Lee, J., Zhu, Y., Seshia, A., Room temperature electrometry with sub-10 electron charge resolution, J Micromech Microeng 18 (2008), 025033.

[12] Shu, W., Laue, E. D., Seshia, A. A., Investigation of biotin-streptavidin binding interactions using microcantilever sensors, Biosens. Bioelectron. 22 (2007), 2003–2009.

[13] Keighley, S. D., Li, P., Estrela, P., Migliorato, P., Optimization of DNA immobilization on gold electrodes for label-free detection by electrochemical impedance spectroscopy, Biosens. Bioelectron 23 (2008), 1291-1297.

[14] Janek, R. P., Fawcett W. R., Impedance Spectroscopy of Self-Assembled Monolayers on Au(111): Sodium Ferrocyanide Charge Transfer at Modified Electrodes, Langmuir 14 (1998), 3011-3018.

[15] Sivasankar, S., Subramaniam, S., Leckband, D., Direct molecular level measurements of the electrostatic properties of a protein surface, Electroanalysis 12 (1998), 12961–12966.

[16] Edmiston, P. L., Saavedra, S. S., Molecular Orientiation Distributions in Protein Films. 4. A Multilayer Composed of Yeast Cytochrome c Bound through an intermediate Streptavidin Layer to a Planar Supported Phospholipid Bilayer, J. Am. Chem. Soc. 120 (1998), 1665-1671.

[17] Caswell, K. K., Wilson, J. N., Bunz, U. H. F., Murphy, C. J., Preferential End-to-End Assembly of Gold Nanorods by Biotin-Streptavidin Connectors, J. Am. Chem. Soc. 125 (2003), 13914-13915.

[18] Fritz, J., Cooper, E., Gaudet, S., Sorger, P., Manalis, S., Electronic detection of DNA by its intrinsic molecular charge, Proc. Natl. Acad. Sci. U. S. A. 99 (2002), 14142-14146.

List of Figures

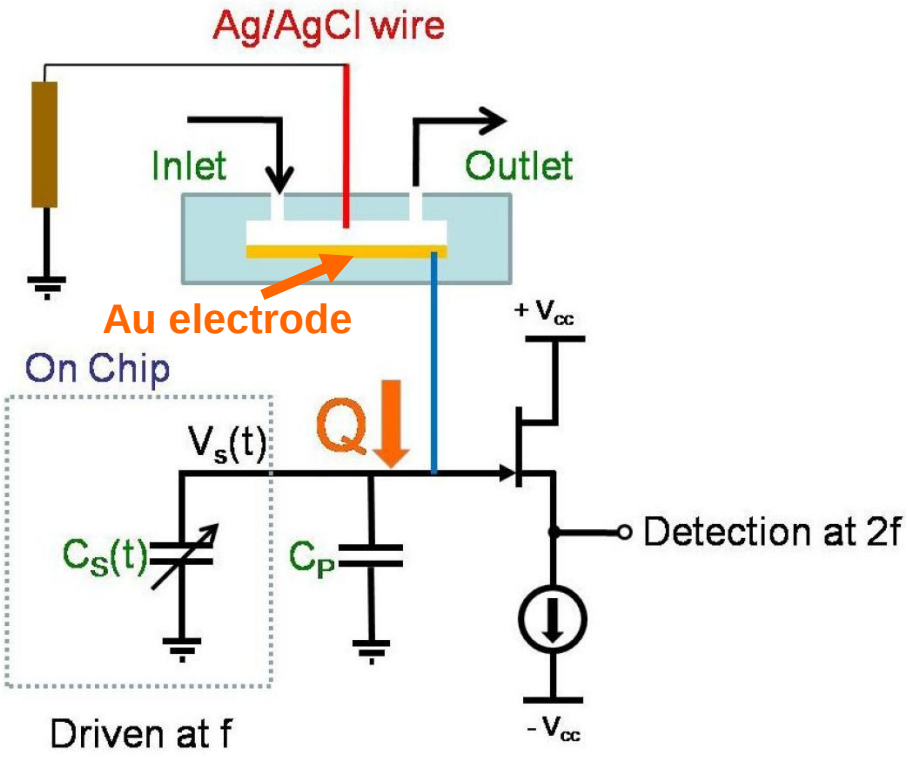
Ag/AgCl wire
Inlet
Outlet
Au electrode
On Chip
+ Vcc
Q
Vs(t)
Cs(t)
CP
Detection at 2f
Driven at f
- Vcc

(a)

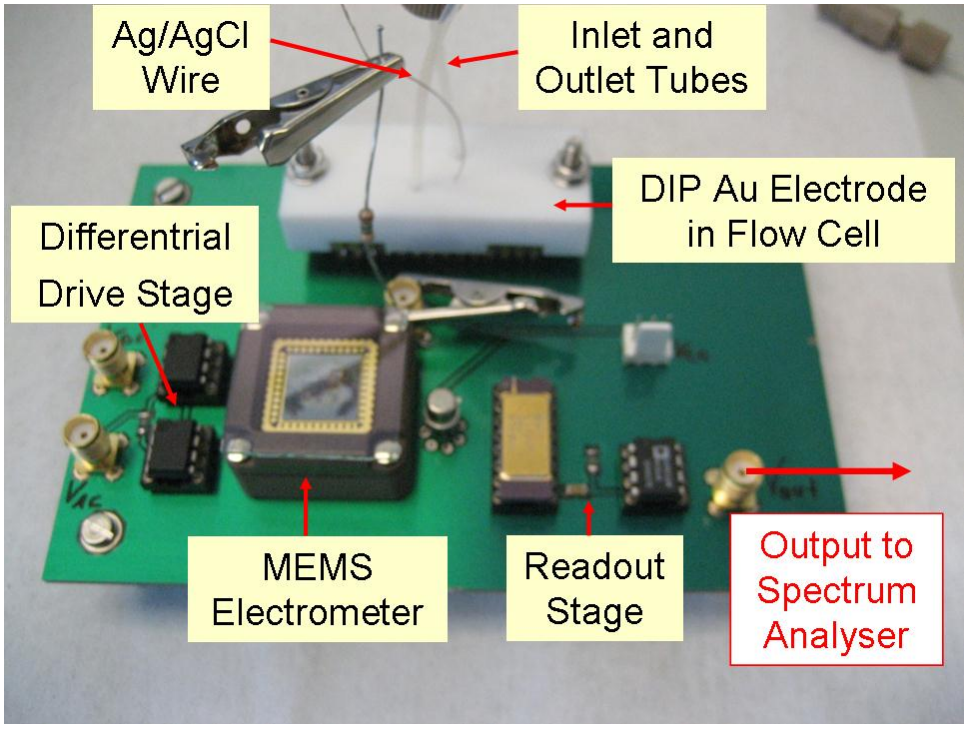
Ag/AgCl Wire
Inlet and Outlet Tubes
DIP Au Electrode in Flow Cell
Differentrial Drive Stage
MEMS Electrometer
Readout Stage
Output to Spectrum Analyser

(b)

Fig. 1

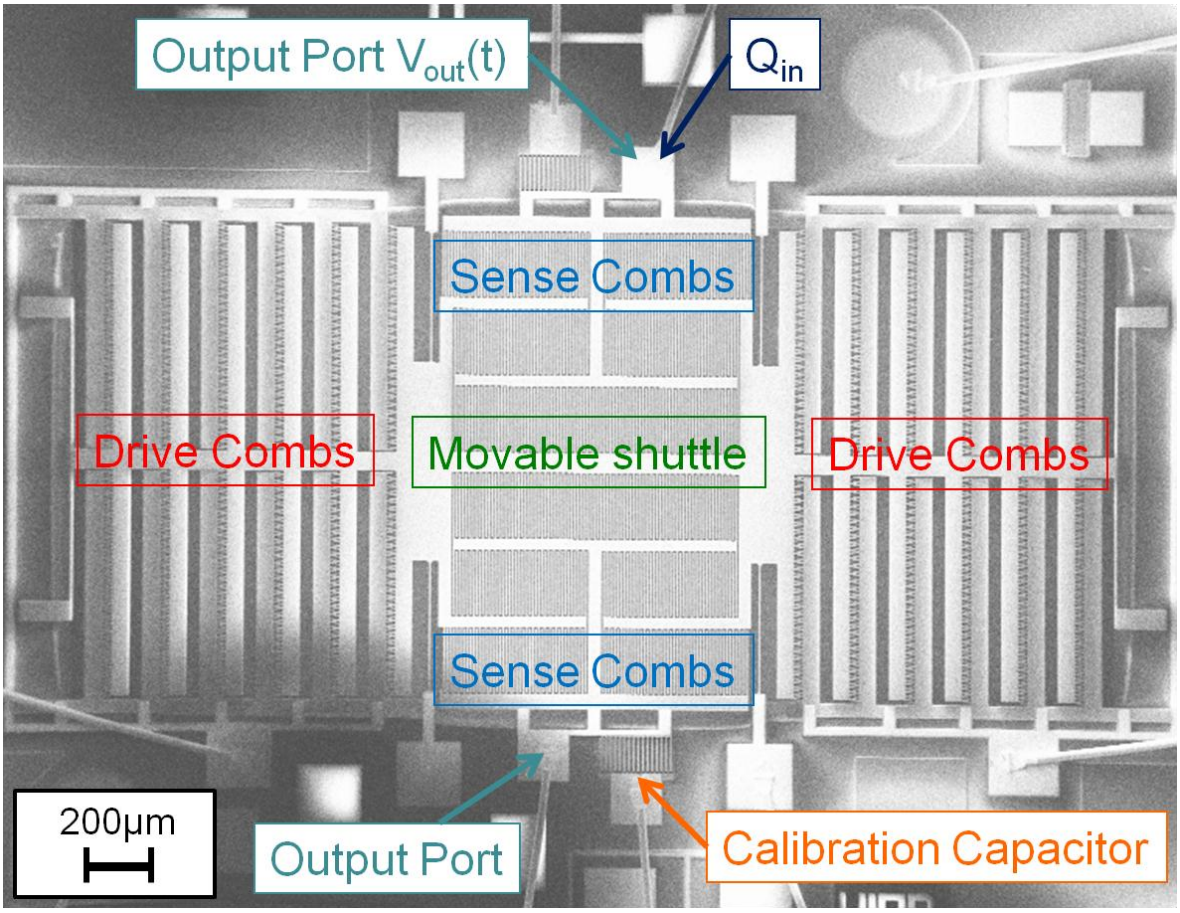
Output Port $V_{out}(t)$
Q_{in}
Sense Combs
Drive Combs
Movable shuttle
Drive Combs
Sense Combs
200µm
Output Port
Calibration Capacitor

Fig. 2

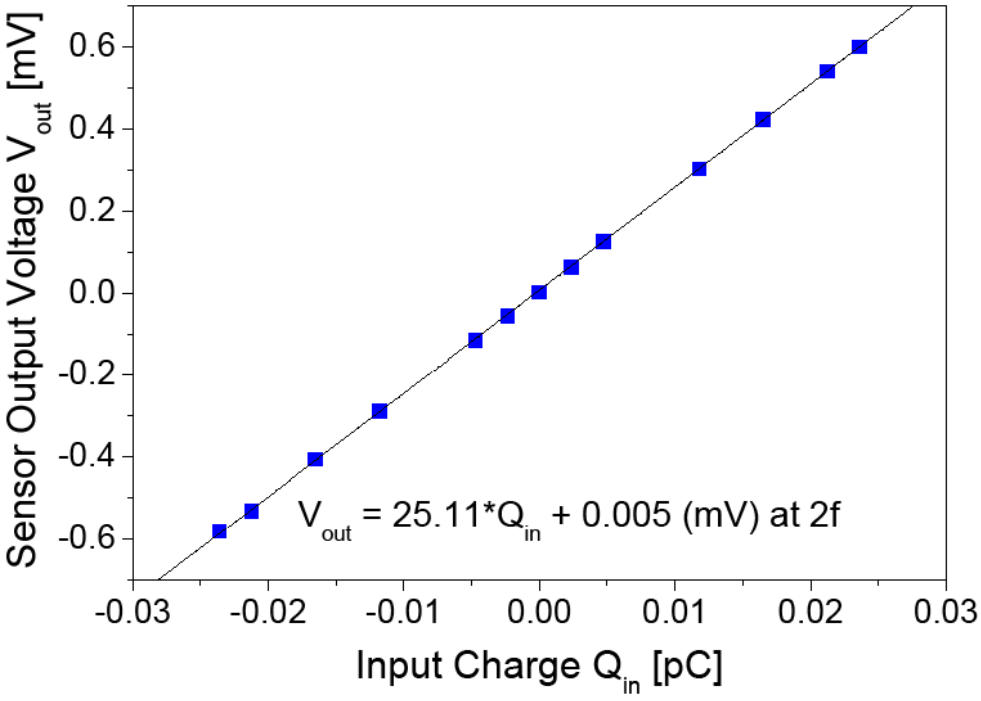
Sensor Output Voltage V_{out} [mV]
0.6
0.4
0.2
0.0
-0.2
-0.4
-0.6
V_{out} = 25.11*Q_{in} + 0.005 (mV) at 2f
-0.03
-0.02
-0.01
0.00
0.01
0.02
0.03
Input Charge Q_{in} [pC]

Fig. 3

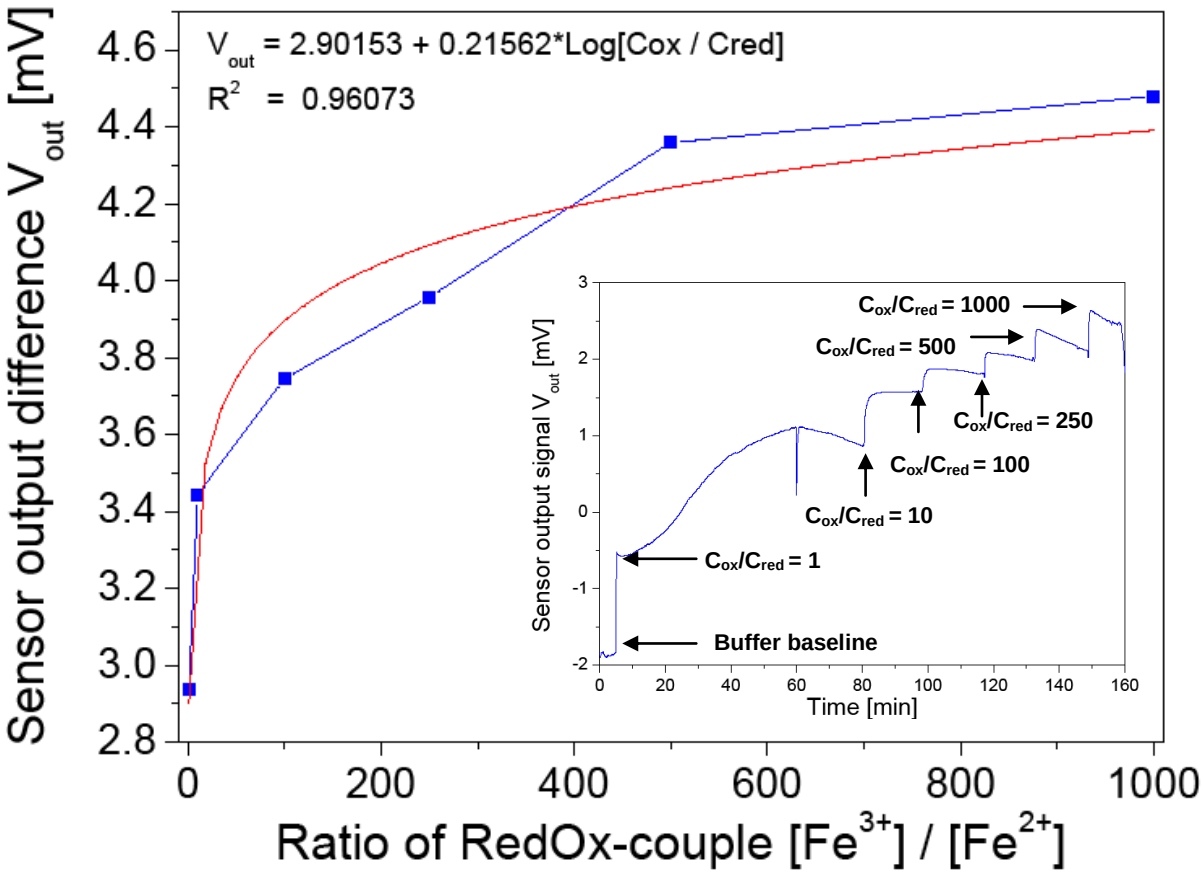
V out = 2.90153 + 0.21562*Log[Cox / Cred]
R2 = 0.96073
Sensor output difference V out [mV]
Ratio of RedOx-couple [Fe3+] / [Fe2+]
Sensor output signal V out [mV]
Time [min]
Cox/Cred = 1000
Cox/Cred = 500
Cox/Cred = 250
Cox/Cred = 100
Cox/Cred = 10
Cox/Cred = 1
Buffer baseline

Fig. 4

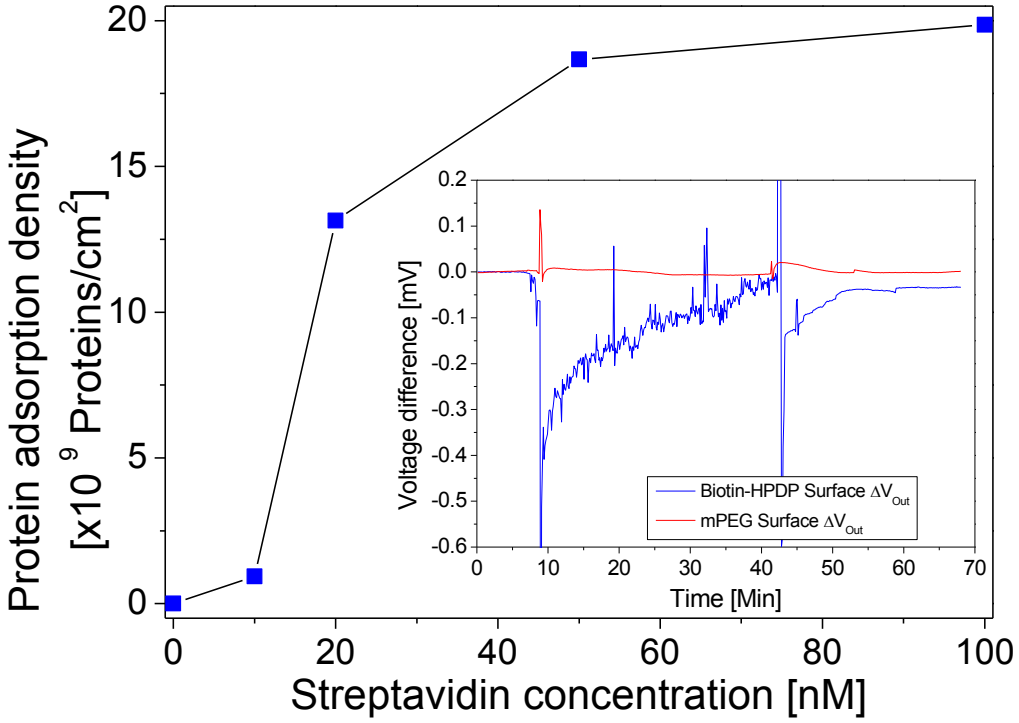
Protein adsorption density
[x10 9 Proteins/cm2]
Streptavidin concentration [nM]
Voltage difference [mV]
Time [Min]
Biotin-HPDP Surface ΔVOut
mPEG Surface ΔVOut

(a)

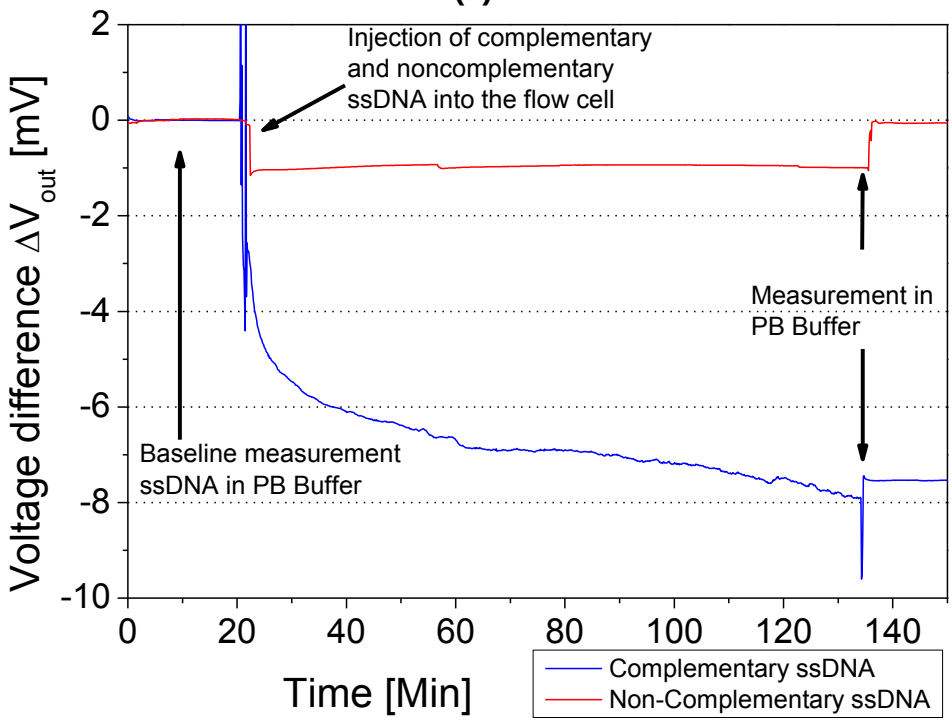
Voltage difference ΔVout [mV]
Time [Min]
Injection of complementary
and noncomplementary
ssDNA into the flow cell
Measurement in
PB Buffer
Baseline measurement
ssDNA in PB Buffer
Complementary ssDNA
Non-Complementary ssDNA

(b)

Fig. 5